Available online at www.sciencedirect.com
SCIENCE DIRECT
Journal of Power Sources 158 (2006) 254–262
JOURNAL OF POWER SOURCES
www.elsevier.com/locate/jpowsour

Durability of $(Pr_{0.7}Sr_{0.3})MnO_{3\pm\delta}$/8YSZ composite cathodes for solid oxide fuel cells

Ke An [a,*], Kenneth L. Reifsnider [b], Carrie Y. Gao [c]

[a] *Metal and Ceramic Division, Oak Ridge National Laboratory, Oak Ridge, TN 37831, USA*
[b] *Connecticut Global Fuel Cell Center, University of Connecticut, Storrs, CT 06269, USA*
[c] *Department of Chemical Engineering, University of Tennessee, Knoxville, TN 37996, USA*

Received 22 June 2005; received in revised form 15 August 2005; accepted 31 August 2005
Available online 19 October 2005

Abstract

Half cell SOFCs with $(Pr_{0.7}Sr_{0.3})MnO_{3\pm\delta}$/8YSZ composite cathodes on 8YSZ electrolytes were aged up to 1000 h at 1000 °C in air with/without 0.318 A cm^{-2} cathodic polarization. During the aging, the performance of the half cell SOFCs was measured using electrochemical impedance spectroscopy (EIS). After aging, the surface of the composite cathode and the interface between the composite cathode and the electrolyte was investigated with scanning electron microscopy (SEM). Chemical element analysis was performed with energy dispersive X-ray spectroscopy (EDS). The performance of the half cell SOFCs degraded after aging with/without polarization compared to the initial state. The SOFCs had a larger polarization resistance after 1000 h of aging. The cathodic current was shown to have an impact on the performance by slowing down the rate of decrease of polarization resistance of the SOFCs. After aging, the microstructural properties—mean pore size increased and cumulative pore volume decreased, and growth of grains was found on the $(Pr_{0.7}Sr_{0.3})MnO_{3\pm\delta}$ phases.

Keywords: Composite cathode; Durability; Aging; Impedance; SOFCs

1. Introduction

SOFCs have shown high efficiency when operated at elevated temperature and are expected to be a candidate for future power sources of the next generation [1]. In recent years, composite electrodes for solid oxide fuel cells (SOFCs) have been studied widely [2–9]. As a mixture of an ionic conductor and an electronic conductor which increases the total reaction zone of the three-phase boundary (TPB), a composite electrode decreases the activation polarization by providing paths for oxygen ions, electrons, and gaseous species transport [4]. In a fuel cell system using a cathode-YSZ composite cathode, fine-grained YSZ components can create better adhesion between the electrode and electrolyte by connecting the gaps between electronic particles and the YSZ substrate [8]. Therefore, the sintering temperature of interface of the electrode/electrolyte can be lowered to decrease the possibility of formation of high resistive products. An addition of up to 40 wt.% YSZ to the cathode improved its performance as a result of better adhesion to the base electrolyte and sites of TPB increased [7]. Cathode overpotential in solid oxide fuel cells makes a large contribution to the output losses in SOFCs [10–12]. It has been reported that among various Sr-doped rare earth manganites, those incorporating Pr^{3+} ions at the A-site exhibited the highest electrical conductivity and maintained the lowest overpotential values [13]. Some investigations have been done on $(Pr_{1-x}Sr_x)MnO_{3\pm\delta}$ (composite) cathodes [10,14–20]. $(Pr_{1-x}Sr_x)MnO_{3\pm\delta}$ was synthesized with an orthorhombic structure in the range of $x<0.5$ and the electrical conductivity of this compound was one order of magnitude higher than $La_{1-x}Sr_xMnO_3$ at elevated temperature [10]. The nonstoichiometric compound $(Pr_{0.6-y}Sr_{0.4})MnO_{3\pm\delta}$ with $y>0$ exhibited higher conductivity and lower overpotential than the stoichiometric one and the commonly used LSM cathode. When $y=0.05$, i.e. the nonstoichiometric $(Pr_{0.55}Sr_{0.4})MnO_{3\pm\delta}$ had the lowest cathodic overpotential and exhibited the best conductivity [15]. The thermal expansion coefficient and chemical stability of this kind of cathode is compatible with the YSZ solid electrolyte. After 100 h at 1000 °C, the cathode film

* Corresponding author. Tel.: +1 865 214 1899; fax: +1 865 574 3940.
E-mail address: kean@vt.edu (K. An).

0378-7753/$ – see front matter © 2005 Elsevier B.V. All rights reserved.
doi:10.1016/j.jpowsour.2005.08.047

kept a porous structure and was coherent to the YSZ substrate [10].

No durability study on $(Pr_{1-x}Sr_x)MnO_{3\pm\delta}$/8YSZ composite cathode under applied long-term cathodic current has been reported. The aim of the present work is to study the long-term durability of the $(Pr_{1-x}Sr_x)MnO_{3\pm\delta}$/8YSZ composite cathodes on 8YSZ electrolyte substrates with/without polarization at elevated temperature in air. Several samples were aged in air and some of them were applied with constant cathodic current. The change of the cathode performance was measured by electrochemical impedance spectroscopy (EIS) during the process of aging. The microstructure and the chemical analysis were investigated on some samples.

2. Experimental

2.1. Samples

To study the durability of the $(Pr_{1-x}Sr_x)MnO_{3\pm\delta}$/8YSZ composite cathodes, half cell SOFCs were used, which consisted of a composite cathode of $(Pr_{0.7}Sr_{0.3})MnO_{3\pm\delta}$/8YSZ and electrolyte of 8YSZ. The 8YSZ electrolyte substrate was made by tape casting. Button shape electrolyte with a radius about 13 mm was cut after the electrolyte substrate was cured in air over night. A thin layer of cathode mixture of $(Pr_{0.7}Sr_{0.3})MnO_{3\pm\delta}$/8YSZ was applied onto the button substrates by screen painting. After sintering at 1400 °C for 1 h, the composite cathode layer was approximately 15–20 μm thick and 20 mm in diameter and the 8YSZ substrate was 180 μm thick.

2.2. Long-term aging and electrochemical measurements

The half cell SOFCs 1 and 2 were half pieces from a single half cell SOFC as received and half cell SOFC2 was aged in air 935 h without any extra pre-processing. The half cell SOFC 3, 4 and 5 were all painted with platinum and aged together. The platinum paste (Structure Probe Inc.) was applied on both sides and covered by a set of platinum gauzes (100 mesh, 0.0762 mm diameter wire, 99.9%, Alfa Aesar) as current collectors. After being painted with the platinum paste and covered with the platinum mesh, the working area of the button SOFCs was about 3.14 cm^2. The schematic configuration of dc or ac impedance measurements is shown in Fig. 1. Aging experiments were run in air in a digitally controlled furnace (Omega LMF-3550). In the furnace, pure platinum wires of 0.381 mm (0.015 in.) diameter were welded onto the platinum gauzes. The half cell SOFCs were held in a specific kind of alumina ceramic holder with spider-web surfaces as shown in Fig. 2. The platinum leads coming out from two-hole alumina ceramic tubes on the holders went together through four-hole alumina ceramic tubes extending through the top of the furnace to lower induction effects during high frequency impedance measurements. Outside the furnace, shielded wiring was used to decrease noise.

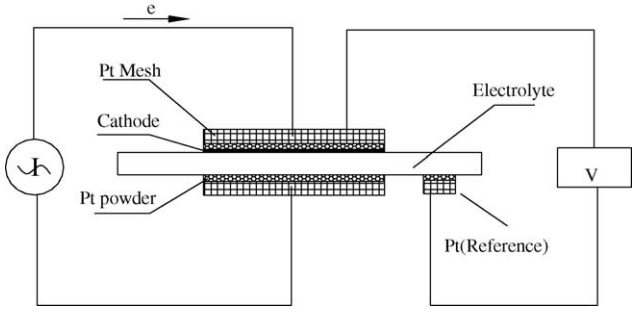

Fig. 1. Schematic configuration of durability measurement.

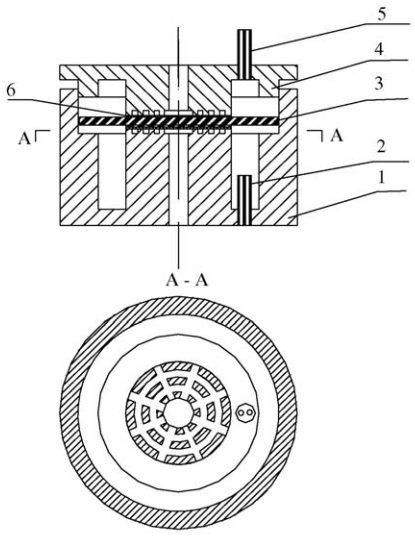

1. bottom Ceramic holder, 2. 2-hole ceramic tube, 3. half cell fuel cell, 4. top ceramic cap, 5. 2-hole ceramic tube, 6. current collector.

Fig. 2. Half cell aging holder.

The elevated temperature was up to 1000 °C. Heating and cooling rates were controlled at 2 °C min^{-1} below 600 °C and 5 °C min^{-1} above 600 °C, respectively. The hold time at elevated temperature was up to 1000 h. At the desired temperatures, measurements were not performed until half an hour delay to achieve stabilization of the temperature. For the button SOFCs aged with applied current, a constant current value of 1 A or about 0.318 A cm^{-2} was applied from the counter electrode to the working electrode using a Keithley 2440 SourceMeter. Impedance measurements were performed by using instruments from Solartron (1260 Impedance Gain-Phase Analyzer + 1287 Electrochemical Interface). Impedance at different temperatures was measured before and after the aging. The impedance measurements during the aging were performed approximately every 100 h. The highest frequency used in the impedance measurements was 10^6 Hz and the lowest was 0.1 Hz. The experimental details for the tested SOFCs are listed in Table 1.

2.3. Microstructure and chemical analysis

The microstructure of the composite cathode surface and the cathode/electrolyte interface was examined by scanning electron microscopy (SEM) and X-ray analysis was performed with energy dispersive X-ray spectroscopy (EDS). Brunauer–Emmett–Teller (BET) tests were run on the samples of half cell SOFC 1 and 2. After being broken into small pieces,

Table 1
Aging test for the half cell SOFCs

Name	Half SOFC 1[a]	Half SOFC 2[a]	Half SOFC 3	Half SOFC 4	Half SOFC 5
Aging time (h)	0	935	1000	1000	1000
Current load (A)	N/A	No	No	1 after 500 h	1
V–time curve	N/A	N/A	N/A	No	Yes
EIS	N/A	No	No	Yes	Yes

N/A: not applicable.
[a] Cells 1 and 2 were half pieces from a single half cell SOFC as received.

the samples were subjected to the BET test with a Sorptomatic 1990 B.E.T system and the data were analyzed using Advanced Data Processing 4.0.

3. Results and discussion

3.1. Durability test

In Fig. 3, the half cell potential voltage and polarization resistance evolutions with time for half cell SOFC 5 are shown. The polarization resistance was measured at low overvoltage, when the current–voltage curves are assumed to be linear. During the test, those unusual voltage peaks in the plot were due to unexpected power outage or other interruptions. Total half cell potential changes of 0.353 V was found for half cell SOFC 5 after the durability test.

3.2. BET

The calculated BET surface area was 0.46 and 0.18 $m^2\ g^{-1}$ for half cell SOFC 1 (as received) and 2 (aged in air 935 h), respectively. The mean pore widths predicted by the Cranston model were 225.5 and 292.3 nm, and the cumulative pore volumes were 0.211 and 0.165 $cm^3\ g^{-1}$ for half cell SOFC 1 and 2, respectively. The predicted result illustrated that the volume percentage of a large amount of nano-scale pores was decreased after long-term aging, which is possible for high temperature sintering of porous materials.

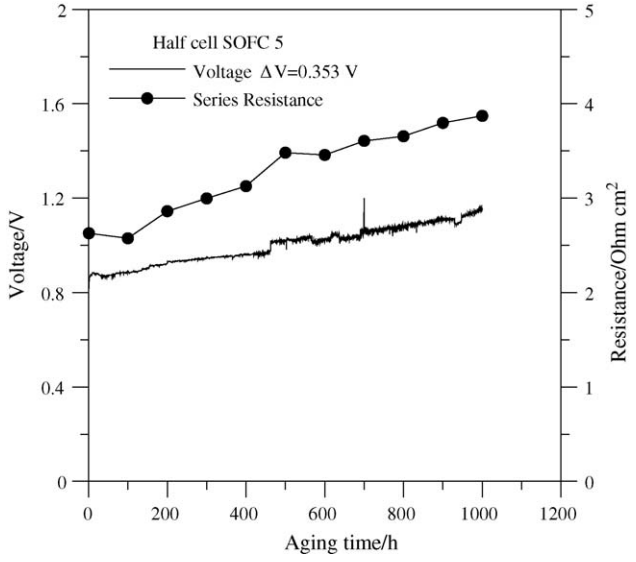

Fig. 3. Voltage evolution during aging for half cell SOFC 5.

3.3. SEM/EDS investigations

3.3.1. SEM

The SEM photos of the cathode surfaces are shown in Fig. 4. Fig. 4a shows the cathode surface of SOFC 1 as received. The multifaceted particles are $(Pr_{0.7}Sr_{0.3})MnO_{3\pm\delta}$ grains and the smooth ones are 8YSZ. From Fig. 4c and d, after aging, the shape of $(Pr_{0.7}Sr_{0.3})MnO_{3\pm\delta}$ grains on the aged half cell SOFCs 3 and 4 was different from the others. Small grains grew on the multifaceted $(Pr_{0.7}Sr_{0.3})MnO_{3\pm\delta}$ grains on the two half cells. This kind of grain growth is not apparent on the surface of half cell SOFCs 2 and 5. EDS tests on the grains did not indicate a significant difference between the aged and unaged half cell SOFCs. For the first 500 h of aging, half cell SOFC 4 was aged in air without current as half cell SOFC 2 and half cell SOFC 3, but it was aged with current for the next 500 h. Half cell SOFC 2 just was as received without being covered with the Pt paste. The existence of the Pt paste may have a catalytic influence on the growth of the small grains. However, the current load may inhibit their growth, since there were not many small grains growing on the surface of half cell SOFC 5, which was applied current all the way during aging.

After the durability test, when half cell SOFCs 4 and 5 were taken out of the specimen holder, it was found that the some areas of the cathodes were delaminated from the electrolyte substrate and adhered to the platinum meshes as they were separated. A view of the electrolyte substrate with the cathode debris due to delamination for SOFC 5 is given in Fig. 4f. From the SEM of the electrolyte substrate, it is easily seen that on some of the delaminated area, where the grain boundaries of the 8YSZ are clear, the 8YSZ particles in the composite cathode were not sintered well with the 8YSZ electrolyte substrate. Similar results have been seen for the electrolyte substrate of half cell SOFC 4. The coefficient of thermal expansion for $(Pr_{0.7}Sr_{0.3})MnO_{3\pm\delta}$ was found to be over $11.5 \times 10^{-6}\ K^{-1}$ [18] and in this study it was measured as $10.8 \times 10^{-6}\ K^{-1}$ for the electrolyte and an average value of $11.0 \times 10^{-6}\ K^{-1}$ for the composite cathode. If the composite cathode was not mixed completely or the 8YSZ particles in the composite were not sintered well with the electrolyte substrate, the thermal stresses might result in delamination during the durability test. On the delaminated 8YSZ substrate surfaces, some area with non-smooth surface was found. This non-smooth area dominated where the 8YSZ powders left on the surface

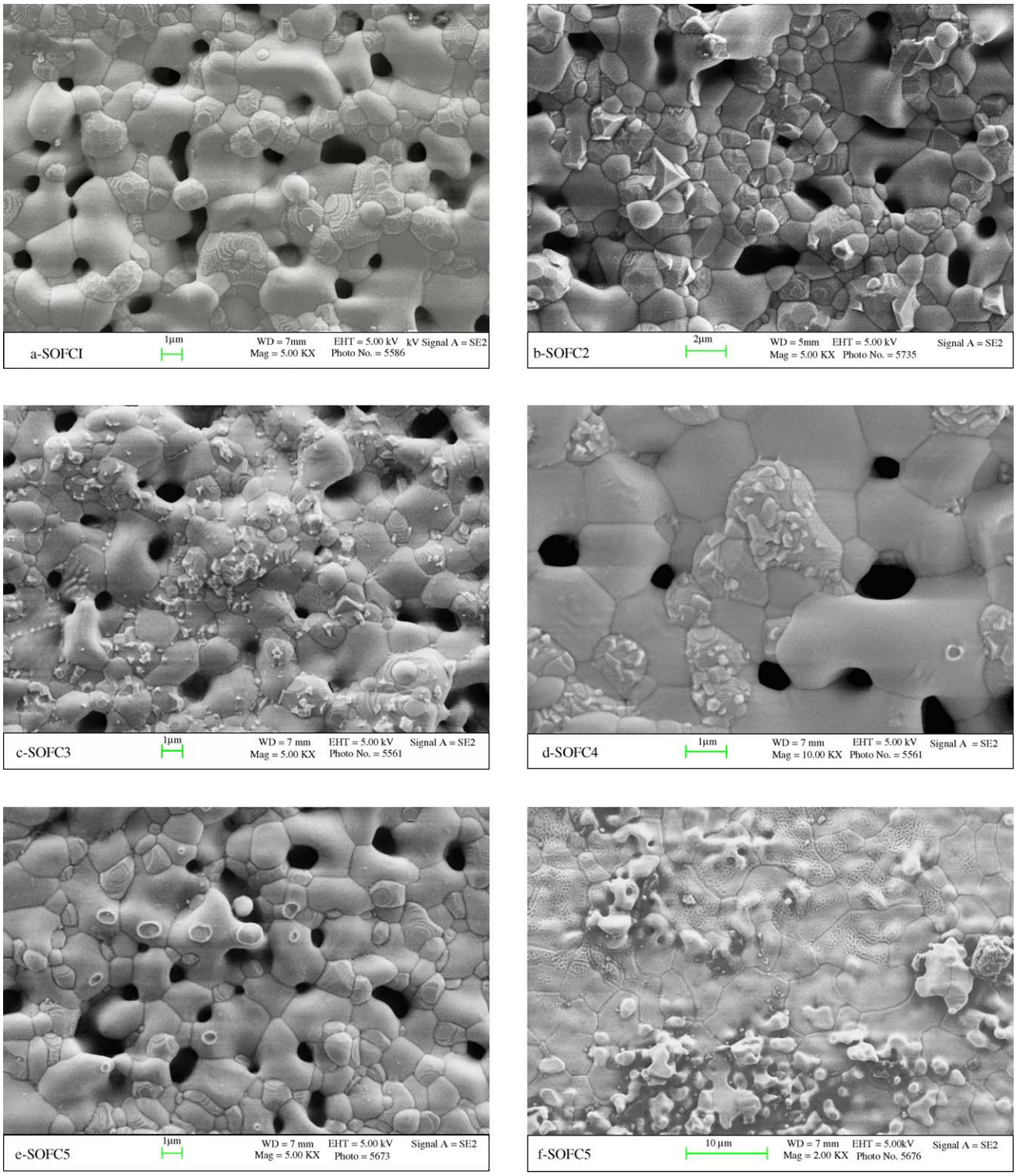

Fig. 4. (a–e) Cathode surface of half cell SOFCs; (f) electrolyte substrate of half cell SOFC 5 with cathode debris.

were sparse. In this region, there could be some delamination between the cathode/electrolyte interface from the fabrication of the fuel cell, or from the delamination as an effect of aging where the composite cathode powders were not sintered strongly onto the electrolyte substrate. Thermodynamically unstable surfaces could attempt to reduce the surface free energy to form this non-smooth grain surface [21].

3.3.2. EDS

On the cross sections of SOFCs 1, 3, 4 and 5, EDS tests were performed on the electrolyte substrate with a series of examinations at a distance of 5, 20 and 50 μm from the interface. The data at the distance of 0 μm was taken from the surface of the electrolyte substrate after delamination for SOFCs 4 and 5. Some elemental traces of Pr, Sr and Mn were found

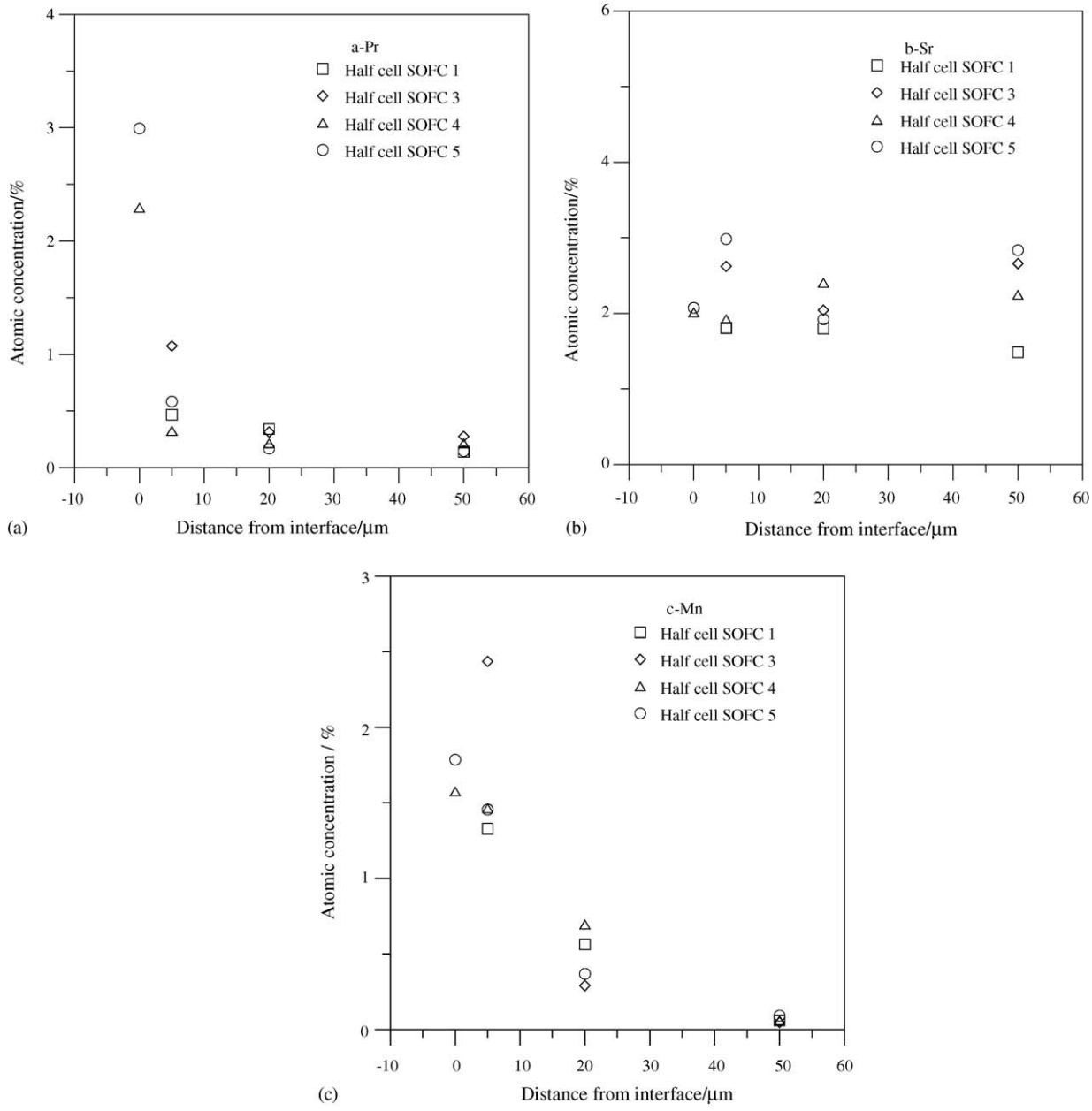

Fig. 5. Cathode elements atomic concentration on the cross sections of the electrolyte substrate.

in the electrolyte substrate. The atomic concentrations of Pr, Sr and Mn are shown in Fig. 5. The atomic concentrations of Pr and Mn were found to be higher close to the interface than inside the electrolyte for all of the samples tested. As deep as 50 μm into the electrolyte, the concentrations were almost 0. The atomic concentrations of Sr were distributed randomly with distance in these SOFCs. No other apparent difference in the concentrations was found for SOFCs tested with and without current. This work shows that the concentration distribution of the cathode material in the electrolyte was not the result of long-term aging, but was the result of making the interface, since the cathode elements were found similarly in the unaged SOFC 1.

3.3.3. Impurities

Impurities were found from the cathode to the electrolyte. The dark particles were found distributed on the delaminated interfaces as shown in Fig. 4f. Inside the electrolyte substrate, impurities were also detected. EDS results indicated the existence of Na, K, Ca, Cl and O, etc. in those dark particles. These impurities may come from raw materials involved in making the SOFCs. Their existence may lead to some of the degradation of performance of the SOFCs by blocking the pores, decreasing the total conductivity and increasing the possibility of delamination of the interface. They also could weaken the strength of the electrolyte by initializing cracks, etc.

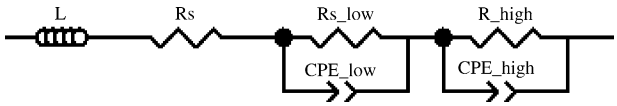

Fig. 6. Equivalent circuit for the impedance measurement.

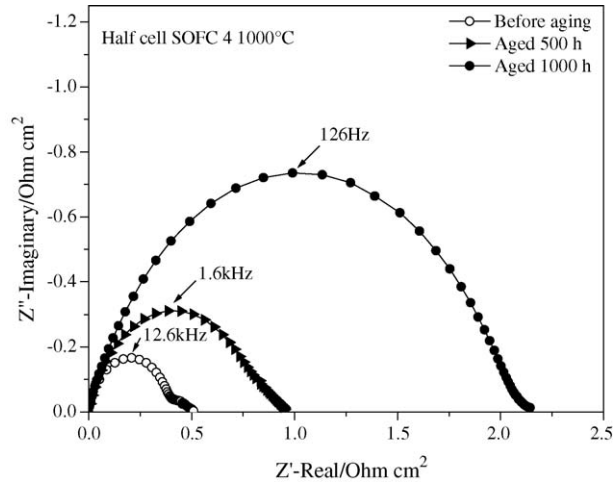

Fig. 7. Impedance spectra for half cell SOFC 4 before and after aging.

3.4. Impedance measurement

The equivalent circuit used for fitting the impedance data is shown in Fig. 6. *L* is an inductor, *R* is a resistor and CPE is a constant phase element [22]. The ohmic resistance R_s part, which is mainly ascribed to the electrolyte, was subtracted and shown in the Nyquist plots. The impedance spectra measured before and after the galvanostatic durability test of the cathodes on half cell SOFCs 4 and 5 are shown in Figs. 7 and 8, respectively. Both SOFCs had a larger polarization resistance after 1000 h of aging. The arcs at lower frequency excitations of the SOFCs were not seen when the polarization resistances were large after aging. If we ignore the process of aging, the polarization resistance of half cell SOFC 4 has apparently increased after being polarized with the 1 A current load for 500 h.

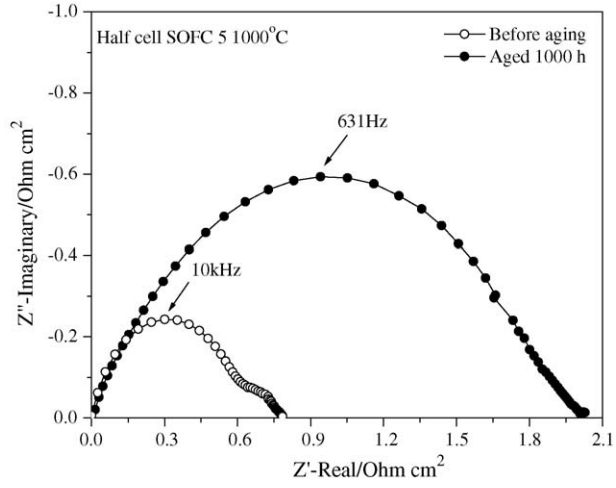

Fig. 8. Impedance spectra for half cell SOFC 5 before and after aging.

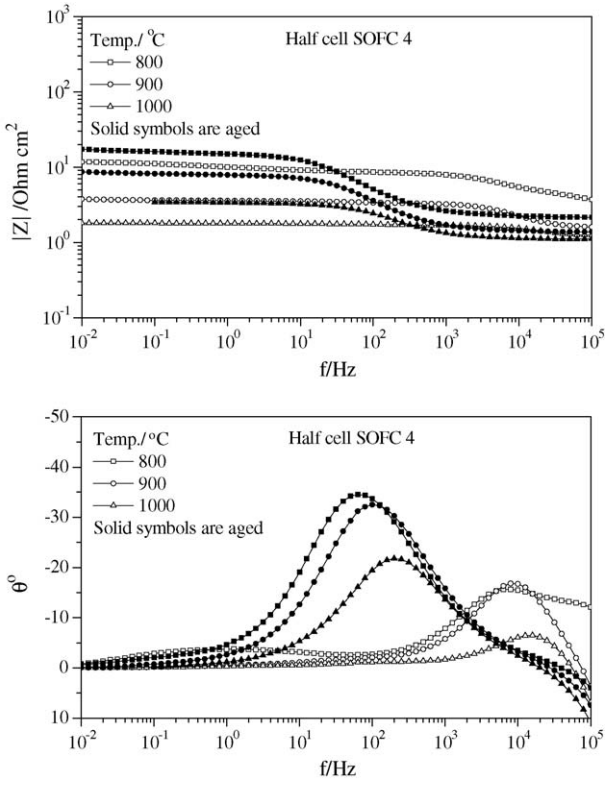

Fig. 9. Bode plot of half cell SOFC 4 at different temperatures.

The influence of the working temperature on the impedance for half cell SOFC 4 and half cell SOFC 5 before and after aging is shown in Figs. 9 and 10. The data are shown in Bode plots from 800 to 1000 °C with intervals of 100 °C. Before aging, the Bode plots of both SOFCs were similar. At a lower temperature of 800 °C two peaks were visible in the Bode plots of phase, but only one impedance peak was visible at higher temperatures. The peaks shifted with the temperature. The effect of temperature was more pronounced at high frequencies than that at low frequencies. After aging, the peaks at lower frequencies and temperature were no longer visible. The peaks at higher frequency shifted to a lower frequency. The peaks for half cell SOFC 4 occurred from 50 to 100 Hz, while for half cell SOFC 5 they were seen in the range from 200 to 700 Hz. Similar impedance results were reported for the LSM/YSZ composite cathode and YSZ electrolyte SOFCs at temperatures from 800 to 1050 °C [23]. That two peaks were visible suggested that the LSM/YSZ cathode had at least two limiting processes [23,24]. The high frequency arc/peak can be attributed to the migration and diffusion of oxygen species from the three-phase boundary region into the electrolyte. The low frequency arc/peak can be attributed to concentration impedance associated with dissociative adsorption and diffusion of oxygen on the cathode surface. Before aging the peaks occurred at lower frequency and temperature was not influential (at higher temperature) because the concentration diffusion polarization of oxygen was negligible when the diffusivity increases with temperature. After aging, the reaction process had been affected. The impedance behavior was similar to that for the mixed ionic and electronic conducting

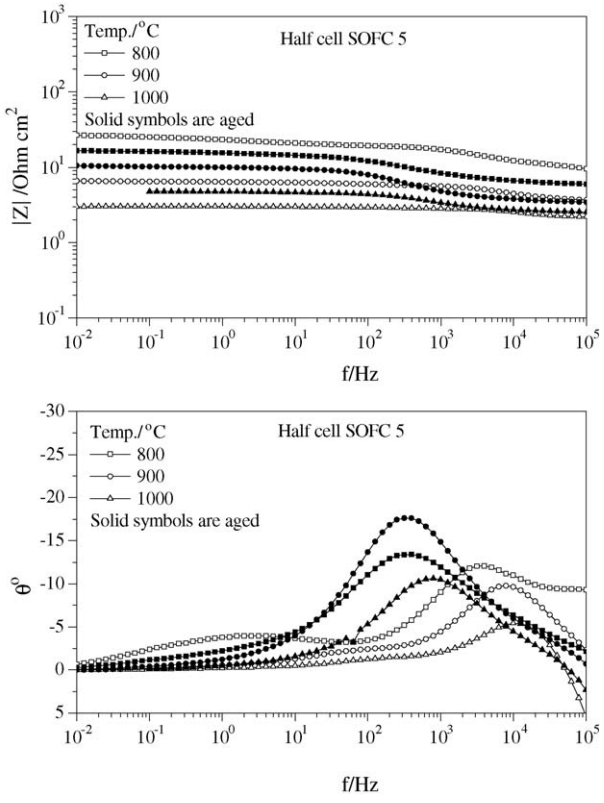

Fig. 10. Bode plot of half cell SOFC 5 at different temperatures.

electrodes such as (LaSr)(CoFe)O_3 [25] and $La_{1-x}Sr_xCoO_{3-d}$ [26,27].

The impedance spectra evolutions with time measured for the cathodes on the half cell SOFCs 4 and 5 are shown in Figs. 11 and 12, respectively. In the parentheses, the frequency of the point with the maximum absolute imaginary value is given. The time dependence of the ohmic resistance R_s, and the polarization resistance R_p ($R_p = R_{low} + R_{high}$) were calculated from the data using the equivalent circuit and were plotted in Figs. 13 and 14, respectively.

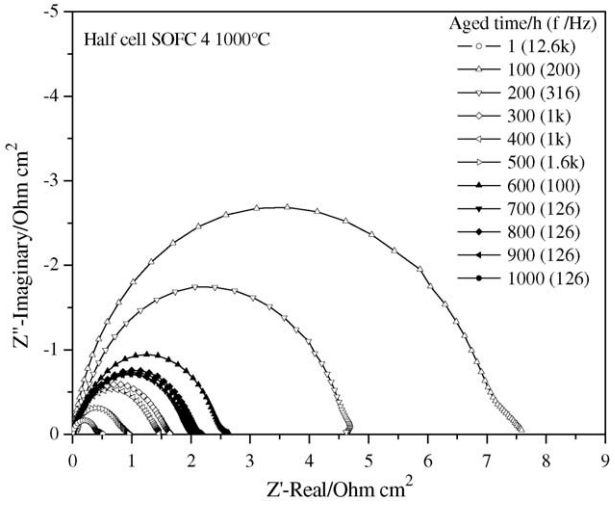

Fig. 11. Impedance spectra evolution for half cell SOFC 4 during aging.

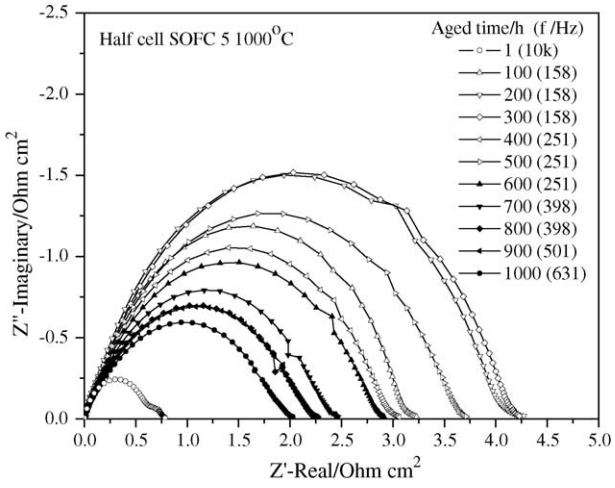

Fig. 12. Impedance spectra evolution for half cell SOFC 5 during aging.

As discussed above for the Bode plots, the high frequency arcs are apparent in the impedance spectra. The R_{high} part has more contribution to the value of R_p than the R_{low} part. After a few hundred hours of aging time, the polarization resistance R_p increased from 0.6 to 6.9 ohm cm^2 for SOFC 4 and from 0.8 to 4.8 ohm cm^2, respectively, with a slight drop of R_s compared to that at the initial state of the SOFCs. The current should not have had an effect on this because this happened to both SOFCs. These changes might come from the migration of impurities to the interface and TPB sites [28], and from the increasing contact area between the platinum mesh and the SOFCs. Since there was no data collected during the first 100 h, it is hard to point out exactly how the process was occurring.

For half cell SOFC 4, before the current was applied, the SOFC performance was increasing with aging time. After it was applied with the current, the value of polarization resistance

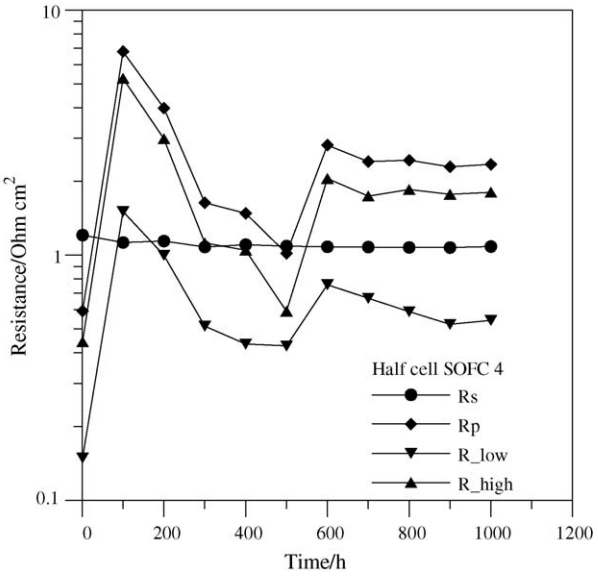

Fig. 13. R_s and R_p resistance with time for half cell SOFC 4.

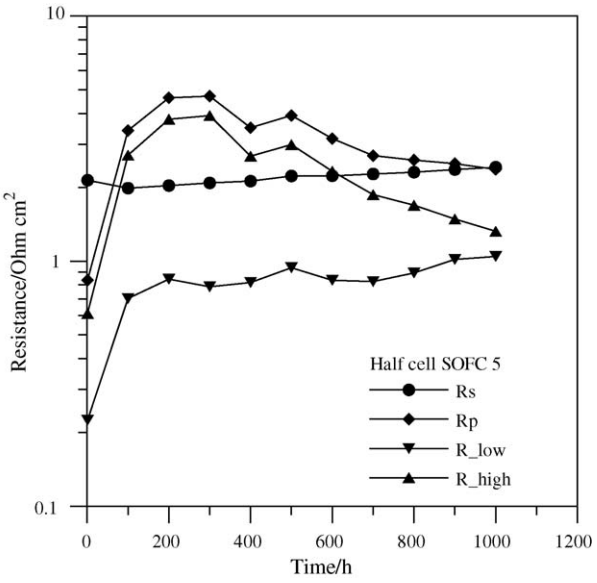

Fig. 14. R_s and R_p resistance with time for half cell SOFC 5.

increased for both the low and high frequency parts with the excitation of polarization aging for the first 100 h. Then the polarization resistance decreased but with lower rate compare to the first 500 h aging without current. With the applied current load, the polarization resistance of half cell SOFC 5 kept decreasing after hitting a peak at around 200 h aging time. However, the low frequency part R_{low} increased little with time. The BET study discussed before indicated that the total volume of pores was reduced. This would effect the oxygen diffusion and concentration and increase the R_{low} part of the polarization resistance. The huge drop of the polarization for the first 500 h of aging of half cell SOFC 4 may be attributed to the growth of the small grains on the multifaceted $(Pr_{0.7}Sr_{0.3})MnO_{3\pm\delta}$ grains thereby increasing the total length of TPB and adsorption area for oxygen. Compared with the possible pore volume change, this increase had a larger contribution to the performance of the SOFC. From the result of half cell SOFC 4, sudden changes of the cell operation parameters during the test had more of an impact on the cell performance than the activation of the cathode from the cathodic current. From the calculated polarization contributions and the rate limiting processes [29], the adsorption, diffusion and charge transfer performance were affected by the current load. However, after long test duration, these effects were compensated to some degree by the microstructure surface changes such as the growth of granular grains and the decrease of the nano-scale pores. However, the R_p could not reach the initial state. As seen for both SOFCs, during the final part of 400 h aging period, the rate of decrease of the polarization resistance reduced. We note that in a study of the long-term performance degradation of button cells consisting of standard materials (LSM, YSZ and Ni/YSZ) [30], thermal cycling tests were conducted first between 312 and 649 h, and at 1321 h a special potential-accelerated aging was applied to the cathode. The dc polarization curves indicated that the potential-accelerated aging caused a large increase in polarization due to an increase of interfacial resistance.

4. Conclusion

After aging in air, for the composite cathodes studied here, the volume of pores was reduced due to the decrease of the amount of nano-scale pores. Growth of small grains was found on the $(Pr_{0.7}Sr_{0.3})MnO_{3\pm\delta}$ phases. Some cathode chemical elements such as Pr and Mn were found in the electrolyte substrate after the SOFCs were sintered. No increasing atomic concentrations were found for them after long-term aging. The gradual decrease of the polarization after a couple of hundred hours aging time may be ascribed to the microstructural surface change thereby increasing the reaction sites of TPB through the cathode and to the decrease of the amount of nano-scale pores. After hitting the peak value during aging, the decreasing polarization resistance from the cathodes could not compensate sufficiently to recover to the initial performance state of the SOFCs. The current load applied had an impact on the overpotential and slowed down the rate of decrease of the polarization resistance of the SOFCs.

References

[1] G. Hoogers, Fuel Cell Technology Handbook, 1st ed., CRC Press LLC, New York, NY, 2003.
[2] M.J. Jorgensen, P. Holtappels, C.C. Appel, Durability test of SOFC cathodes, J. Appl. Electrochem. 30 (4) (2000) 411–418.
[3] M. Juhl, S. Primdahl, C. Manon, M. Mogensen, Performance/structure correlation for composite SOFC cathodes, J. Power Sources 61 (1–2) (1996) 173–181.
[4] A.V. Virkar, J. Chen, C.W. Tanner, J.-W. Kim, The role of electrode microstructure on activation and concentration polarizations in solid oxide fuel cells, Solid State Ionics 131 (1–2) (2000) 189–198.
[5] T. Kenjo, M. Nishiya, $LaMnO_3$ air cathodes containing ZrO_2 electrolyte for high temperature solid oxide fuel cells, Solid State Ionics 57 (3–4) (1992) 295–302.
[6] S. Wang, Y. Jiang, Y. Zhang, J. Yan, W. Li, Promoting effect of YSZ on the electrochemical performance of YSZ + LSM composite electrodes, Solid State Ionics 113–115 (1998) 291–303.
[7] M.J.L. Ostergard, C. Clausen, C. Bagger, M. Mogensen, Manganite–zirconia composite cathodes for SOFC: influence of structure and composition, Electrochim. Acta 40 (12) (1995) 1971–1981.
[8] J.H. Choi, J.H. Jang, S.M. Oh, Microstructure and cathodic performance of $La_{0.9}Sr_{0.1}MnO_3$/yttria-stabilized zirconia composite electrodes, Electrochim. Acta 46 (6) (2001) 867–874.
[9] J.-D. Kim, G.-D. Kim, J.-W. Moon, Y.-I. Park, W.-H. Lee, K. Kobayashi, M. Nagai, C.-E. Kim, Characterization of LSM–YSZ composite electrode by AC impedance spectroscopy, Solid State Ionics 143 (3–4) (2001) 379–389.
[10] T.-L. Wen, H. Tu, Z. Xu, O. Yamamoto, A study of (Pr, Nd, Sm)$_{1-x}Sr_xMnO_3$ cathode materials for solid oxide fuel cell, Solid State Ionics 121 (1–4) (1999) 25–30.
[11] A.M. Svensson, S. Sunde, K. Nisancioglu, A mathematical model of the porous SOFC cathode, Solid State Ionics 86–88 (2) (1996) 1211–1216.
[12] T. Horita, K. Yamaji, N. Sakai, Y. Xiong, T. Kato, H. Yokokawa, T. Kawada, Imaging of oxygen transport at SOFC cathode/electrolyte interfaces by a novel technique, J. Power Sources 106 (1–2) (2002) 224–230.
[13] T. Ishihara, T. Kudo, H. Matsuda, Y. Takita, Doped $PrMnO_3$ perovskite oxide as a new cathode of solid oxide fuel cells for low temperature operation, J. Electrochem. Soc. 142 (5) (1995) 1519–1525.
[14] G.C. Kostogloudis, N. Vasilakos, C. Ftikos, Preparation and characterization of $Pr_{1-x}Sr_xMnO_{3-\Delta}$ ($X = 0$, 0.15, 0.3, 0.4, 0.5) as a potential SOFC cathode material operating at intermediate temperatures (500–700 °C), J. Eur. Ceram. Soc. 17 (12) (1997) 1513–1521.

[15] X. Huang, J. Liu, Z. Lu, W. Liu, L. Pei, T. He, Z. Liu, W. Su, Properties of nonstoichiometric $Pr_{0.6-x}Sr_{0.4}MnO_3$ as the cathodes of SOFCs, Solid State Ionics 130 (3–4) (2000) 195–201.

[16] A. Naoumidis, A. Ahmad-Khanlou, Z. Samardzija, D. Kolar, Chemical interaction and diffusion on interface cathode/electrolyte of SOFC, Fresen. J. Anal. Chem. 365 (1999) 277–281.

[17] H.-R. Rim, S.-K. Jeung, E. Jung, J.-S. Lee, Characteristics of $Pr_{1-x}M_xMnO_3$ (M = Ca, Sr) as cathode material in solid oxide fuel cells, Mater. Chem. Phys. 52 (1998) 54–59.

[18] Y. Sakaki, Y. Takeda, A. Kato, N. Imanishi, O. Yamamoto, M. Hattori, M. Iio, Y. Esaki, $Ln_{1-x}Sr_xMnO_3$ (Ln = Pr, Nd, Sm and Gd) as the cathode material for solid oxide fuel cells, Solid State Ionics 118 (3–4) (1999) 187–194.

[19] K. An, K.L. Reifsnider, A multiphysics modeling study of $(Pr_{0.7}Sr_{0.3})MnO_{3\pm\delta}$8YSZ composite cathodes for solid oxide fuel cells, ASME J. Fuel Cell Sci. Technol. 2 (2005) 45–51.

[20] H.Y. Tu, Y. Takeda, N. Imanishi, O. Yamamoto, $Ln_{0.4}Sr_{0.6}Co_{0.8}Fe_{0.2}O_{3-\delta}$ (Ln = La, Pr, Nd, Sm, Gd) for the electrode in solid oxide fuel cells, Solid State Ionics 117 (3–4) (1999) 277–281.

[21] K.V. Jensen, R. Wallenberg, I. Chorkendorff, M. Mogensen, Effect of impurities on structural and electrochemical properties of the Ni-YSZ interface, Solid State Ionics 160 (1–2) (2003) 27–37.

[22] B.A. Boukamp, A nonlinear least squares fit procedure for analysis of immittance data of electrochemical systems, Solid State Ionics 20 (1) (1986) 31–44.

[23] M.J. Jorgensen, Lanthanum manganate based cathodes for solid oxide fuel cells, Ph.D. Dissertation, Riso National Laboratory, Denmark, 2001.

[24] S.P. Jiang, Y.J. Leng, S.H. Chan, K.A. Khor, Fabrication of high performance (La, Sr)MnO_3 cathodes by ion impregnation, in: Proceedings of the Eighth International Symposium on Solid Oxide Fuel Cells, The Electrochemical Society, Paris, France, 2003.

[25] S.P. Jiang, A comparison of O_2 reduction reactions on porous (La, Sr)MnO_3 and (La, Sr)(Co, Fe)O_3 electrodes, Solid State Ionics 146 (1–2) (2002) 1–22.

[26] T. Horita, K. Yamaji, N. Sakai, H. Yokokawa, A. Weber, E. Ivers-Tiffee, Oxygen reduction mechanism at porous $La_{1-x}Sr_xCoO_{3-d}$ cathodes/$La0_{.8}Sr_{0.}2Ga_{0.8}Mg_{0.2}O_{2.8}$ electrolyte interface for solid oxide fuel cells, Electrochim. Acta 46 (12) (2001) 1837–1845.

[27] A. Endo, H. Fukunaga, C. Wen, K. Yamada, Cathodic reaction mechanism of dense $La_{0.6}Sr_{0.4}CoO_3$ and $La_{0.81}Sr_{0.09}MnO_3$ electrodes for solid oxide fuel cells, Solid State Ionics 135 (1–4) (2000) 353–358.

[28] V.K. Hansen, M. Mogensen, H_2–H_2O–Ni–YSZ electrode performance and segregation to the interface, in: Proceedings of the Eighth International Symposium on Solid Oxide Fuel Cells, The Electrochemical Society, Paris, France, 2003.

[29] S.P. Jiang, J.G. Love, Y. Ramprakash, Electrode behaviour at (La, Sr)MnO_3/Y_2O_3–ZrO_2 interface by electrochemical impedance spectroscopy, J. Power Sources 110 (1) (2002) 201–208.

[30] Y.C. Hsiao, J.R. Selman, The degradation of SOFC electrodes, Solid State Ionics 98 (1–2) (1997) 33–38.